

Minimalist Probes for Studying Protein Dynamics: Thioamide Quenching of Selectively Excitable Fluorescent Amino Acids

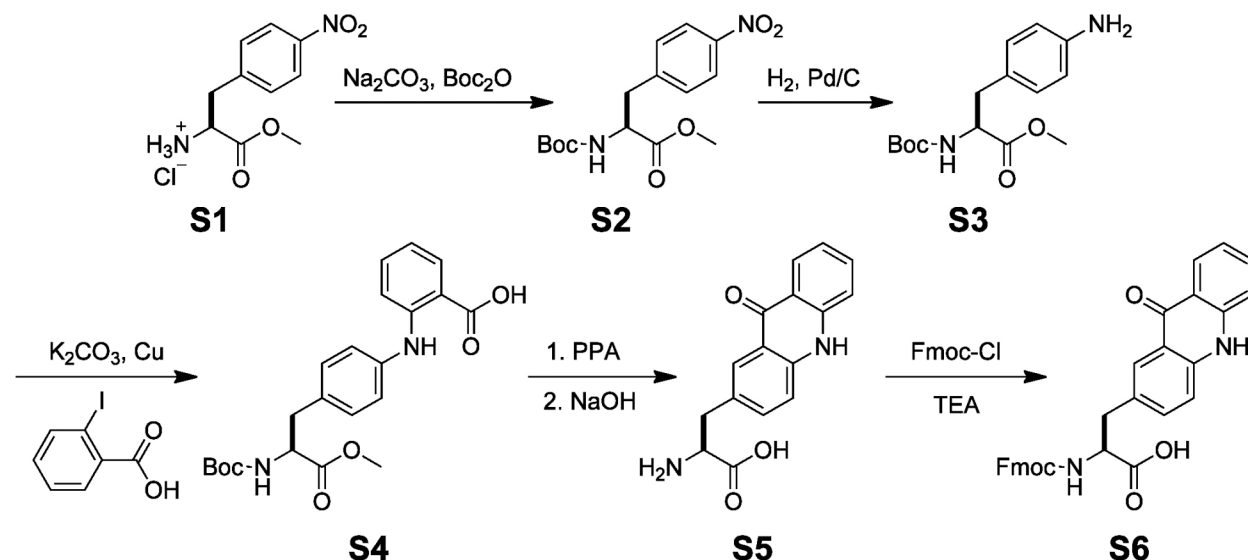
Jacob M. Goldberg, Lee C. Speight, Mark W. Fegley, & E. James Petersson

*Department of Chemistry, University of Pennsylvania
231 South 34th Street, Philadelphia, Pennsylvania 19104-6323 USA.*

General Information. Boc-L-thionoleucine-1-(6-nitro)benzotriazolide and Fmoc- β -(7-methoxycoumarin-4-yl)-Ala-OH were purchased from Bachem (Torrence, CA). Fmoc-L-(7-Aza)Trp-OH was purchased from RSP Amino Acids (Shirley, MA). Rink amide resin, 2-chlorotrityl resin, Fmoc-Ala-OH, Fmoc-Arg(Pbf)-OH, Fmoc-Asn(Trt)-OH, Fmoc-Asp(OtBu)-OH, Fmoc-Glu(OtBu)-OH, Fmoc-Gln(Trt)-OH, Fmoc-Gly-OH, Fmoc-Leu-OH, Fmoc-Lys(Boc)-OH, Fmoc-Met-OH, Fmoc-Phe-OH, Fmoc-Pro-OH, Fmoc-Ser(OtBu)-OH, Fmoc-Thr(OtBu)-OH, Fmoc-Trp(Boc)-OH, and Fmoc-Val-OH were purchased from Novabiochem (San Diego, CA). Piperidine and 2-(1*H*-benzotriazol-1-yl)-1,1,3,3-tetramethyluronium hexafluorophosphate (HBTU) were purchased from American Bioanalytical (Natick, MA). Sigmacote, *N,N*-diisopropylethylamine (DIPEA), 1-methyl-2-pyrrolidinone (NMP), *p*-nitrophenylalanine methyl ester hydrochloride, D, L-7-azatryptophan, 7-methoxycoumarin, and acridone were purchased from Sigma-Aldrich (St. Louis, MO). All other reagents were purchased from Fisher Scientific (Pittsburgh, PA). Milli-Q filtered (18 M Ω) water was used for all solutions (Millipore; Billerica, MA). All glass peptide synthesis reaction vessels (RVs) were treated with Sigmacote prior to use. UV absorbance spectra were obtained with a Hewlett-Packard 8452A diode array spectrophotometer (currently Agilent Technologies; Santa Clara,

CA). Fluorescence spectra were collected with a Varian Cary Eclipse fluorescence spectrophotometer fitted with a Peltier multicell holder (currently Agilent Technologies; Santa Clara, CA). Circular dichroism experiments were conducted with an Aviv 410 CD spectrometer (Aviv Biomedical; Lakewood, NJ). Proton (^1H) and carbon (^{13}C) NMR spectra were collected with a Bruker DRX 500 MHz spectrometer (Billerica, MA). DEPT-135 peaks are indicated parenthetically after ^{13}C chemical shifts. Matrix-assisted laser desorption ionization (MALDI) mass spectra were collected with a Bruker Ultraflex III MALDI-TOF-TOF mass spectrometer. “Low resolution” electrospray ionization (ESI) mass spectrometry (LRMS) was conducted with a Waters Acquity Ultra Performance Liquid Chromatograph outfitted with a single quadrupole detector (SQD) mass spectrometer (Milford, MA). “High resolution” ESI mass spectrometry (HRMS) was conducted with a Waters LCT Premier XE LC/MS.

Chemical Synthesis. Compounds **S2** to **S4** were synthesized essentially as described.^{S1} Characterization matched previous reports.



Scheme S1. Synthesis of Fmoc-acridon-2-yl alanine amino acid. Boc_2O : Di-*t*-butyl dicarbonate, PPA: Polyphosphoric Acid, TEA: Triethylamine

2-amino-3-(9-oxo-9,10-dihydroacridin-2-yl)propanoic acid (Acid-OH, S5). Polyphosphoric acid (3 mL) was added to a flask containing **S4** (0.188 g, 0.454 mmol) and the mixture was heated to 140 °C and stirred magnetically for 2 h. The reaction was removed from heat and allowed to cool to 50 °C. Water (50 mL) was added and the flask was allowed to stand at 4 °C overnight. The resulting yellow precipitate was filtered and washed with cold water. The compound was dried under reduced pressure, then added to 3 mL of water and the pH adjusted to 9 by dropwise addition of 10 M NaOH. After stirring for 2 hours, the mixture was acidified with 6 M HCl to pH 2 and cooled on ice to precipitate product. The resulting solid was collected by vacuum filtration and dried to yield **S5** as a yellow powder (0.081 g; 63 % yield). ¹H NMR (500 MHz, CD₃OD) δ 8.33 (dd, *J* = 1.8, 1.1 Hz, 1H), 8.25 (d, *J* = 1.8 Hz, 1H), 7.75 (m, 1 H), 7.68 (dd, *J* = 8.6, 2.1 Hz, 1H), 7.53 (dd, *J* = 8.5, 3.8 Hz, 2H), 7.3 (m, 1H), 4.28 (dd, *J* = 7.7, 5.4 Hz, 1H), 3.54 (m, 2H); ¹³C NMR (125 MHz, CD₃OD): δ 180.1(no peak), 171.5 (no peak), 142.74 (no peak), 142.28 (no peak), 136.1 (+), 135.3 (+), 129.0 (no peak), 128.3 (+), 127.5 (+), 123.0 (+), 119.6 (+), 119.3 (no peak), 118.6 (+), 117.0 (no peak), 55.3 (+), 37.2 (-); HRMS (ESI) *m/z* calcd for C₁₆H₁₅N₂O₃⁺ [M+H]⁺ 283.1083, found 283.1093.

2-(9H-fluoren-9-ylmethoxycarbonylamino)-3-(9-oxo-9,10-dihydro-acridin-2-yl)-propionic acid (Fmoc-Acid-OH, S6). Triethylamine (TEA) was added dropwise to a solution of **S5** (0.300 g, 1.06 mmol) in water (5 mL) until the pH was approximately 8.5. A solution of 9-fluorenyl methyl chloroformate (0.300 g, 1.16 mmol) in acetonitrile (3 mL) was then added to the reaction and the contents were stirred for 45 min. The reaction was acidified with concentrated HCl until the pH was less than 6. The organics were then extracted with CH₂Cl₂ (3 x 40 mL) and concentrated under reduced pressure to afford **S6** as a yellow solid (0.402 g, 75 % yield). ¹H NMR (500 MHz, DMF-d₇): δ 12.03 (s, 1H), 8.37 – 8.34 (m, 1H) 7.95 – 7.86 (m, 4H), 7.74 (dd, *J*

= 7.4, 0.4 Hz, 2H), 7.71 – 7.63 (m, 1H), 7.46 – 7.36 (m, 4H), 7.33 (td, $J = 7.4, 1.1$ Hz, 3H), 6.31 (s, 1H), 5.81 (s, 1H), 5.04 (s, 1H) 4.25 – 4.20 (m, 1H), 4.1 (t, $J = 7.0$ Hz, 1H), 3.90 (d, $J = 7.0$ Hz, 1H), 3.23 – 3.16 (m, 1H), 1.33 (t, $J = 7.3$ Hz, 1H); ^{13}C NMR (125 MHz, DMF- d_7): δ 177.4, 174.1, 156.4, 145.9, 143.6, 141.5, 140.6, 140.2, 138.2, 131.5, 129.2, 127.9, 127.5, 127.1, 125.7, 121.6, 121.3, 121.2, 121.0, 120.1, 109.1, 64.9, 51.0, 45.9, 8.6; HRMS (ESI) m/z calcd for $\text{C}_{31}\text{H}_{25}\text{N}_2\text{O}_5^+$ $[\text{M}+\text{H}]^+$ 505.1763, found 505.1767; calcd for $\text{C}_{31}\text{H}_{24}\text{N}_2\text{NaO}_5^+$ $[\text{M}+\text{Na}]^+$ 527.1583, found 527.1588.

Peptide Synthesis and Purification. Proline and glycine peptides Leu-Pro₂-7Aw (LP₂ ω), Leu'-Pro₂-7Aw (L'P₂ ω), Leu-Pro₂-Mcm (LP₂ μ), Leu'-Pro₂-Mcm (L'P₂ μ), Leu-Pro₂-Acid (LP₂ δ), Leu'-Pro₂-Acid (L'P₂ δ), Leu-Gly₂-7Aw (LG₂ ω), Leu'-Gly₂-7Aw (L'G₂ ω), Leu-Gly₂-Mcm (LG₂ μ), Leu'-Gly₂-Mcm (L'G₂ μ), Leu-Gly₂-Acid (LG₂ δ), and Leu'-Gly₂-Acid (L'G₂ δ) were each synthesized on a 12.5 μmol scale on 2-chlorotrityl resin. The C-terminal amide peptides Leu-Pro₂-Acid-NH₂ (LP₂ δ -NH₂) and Leu'-Pro₂-Acid (L'P₂ δ -NH₂) were synthesized on a 12.5 μmol scale on Rink amide resin. Since the first three amino acid couplings in each pair of oxo- and thiopeptides are identical, these residues were coupled on a 25 μmol scale in a common pot. The resin was then divided into two equal portions for the final amino acid coupling of either Leu or Leu' and the reagents were scaled accordingly. Acid was incorporated through the Fmoc-protected compound **S6**. For a typical synthesis, 2-chlorotrityl resin (100-200 mesh; 0.6 mmol substitution/g; 25 μmol) was added to a dry RV. Two successive 15 min incubations with 5 mL dimethylformamide (DMF) and magnetic stirring were used to swell the resin. After swelling, DMF was removed with vacuum suction. The first amino acid in DMF (5 equiv; 83 mM, 1.5 mL) and DIPEA (10 equiv; 44 μL) were added to the RV and the mixture was allowed to react for 30 min with magnetic stirring. Spent solution was removed with vacuum suction and the

resin beads were washed thoroughly with DMF. Excess DMF was removed with vacuum suction and the resin beads were deprotected by treatment with 20% piperidine in DMF (5 mL) for 20 min with magnetic stirring. The deprotection solution was drained from the RV and the beads were rinsed extensively with DMF. Subsequent amino acid couplings and deprotections proceeded as described above, with the exception that the remaining Fmoc-protected amino acids were activated with HBTU (5 equiv) prior to addition to each reaction. Since the thioleucine was introduced through the pre-activated Boc-L-thionoleucine-1-(6-nitro)benzotriazolide, HBTU was not added for these couplings. The final N-terminal Fmoc group was removed from the Leu-containing peptides before the peptide was cleaved from the resin. After the beads were washed extensively with DMF and dried with CH_2Cl_2 , peptides were cleaved by successive 60 min and 30 min incubations on a rotisserie with 2.5 mL of a fresh cleavage cocktail of trifluoroacetic acid (TFA), water, and triisopropylsilane (TIPS) (10:9:1 v/v). After each treatment, the resulting solution was expelled from the RV with nitrogen, reduced to a volume of less than 1 mL by rotary evaporation, and diluted with 6 mL of $\text{CH}_3\text{CN}/\text{H}_2\text{O}$ (2:1 v/v). The amidated peptides were synthesized in exactly the same fashion, with the exception that the Rink amide resin (100-200 mesh; 0.6 mmol substitution/g; 25 μmol) was deprotected with 20% piperidine in DMF and HBTU was added to the first coupling reaction. The cleavage cocktail for the amidated peptides was 38:1:1 TFA/ H_2O /TIPS (v/v).

The peptides were purified to homogeneity by reverse-phase HPLC on a Vydac 218TP C18 semi-prep column (Grace/Vydac; Deerfield, IL) using a linear solvent gradient that ranged from 98% to 60% aqueous phase over 19 min, then to 0% aqueous phase over 5 min, then returning to 98% aqueous phase during a 10 min wash out period. MALDI-MS was used to confirm

identities (Table S1). Purified peptides were dried in a vacuum centrifuge (Savant/Thermo Scientific; Rockford, IL).

The villin headpiece subdomain variant HP35-Acd₃₅ (HP35- δ_{35}) has the sequence LSDEDFKAVFGMTRSAFANLPLWKQQNLKKEKGL δ .^{S2} In the thioamide-containing peptide HP35-Leu'₁Acd₃₅ (HP35-L'₁ δ_{35}), the N-terminal leucine is replaced with thioleucine. Each peptide was synthesized on a 25 μ mol scale on 2-chlorotrityl resin using a combination of manual and automated techniques. After the resin was swelled, Fmoc-Acd (compound S6) was loaded onto resin (0.6 mmol substitution/g; 50 μ mol) as described above. After capping unreacted sites with MeOH, the resin was transferred to a 100 μ mol scale microwave reaction vessel and residues Ser₂ – Leu₃₄ were coupled using a Liberty 1 single channel automated peptide synthesizer (CEM Corporation; Matthews, NC). All residues were coupled and deprotected with microwave irradiation and nitrogen bubbling. For each coupling, 2.5 mL of the Fmoc-protected amino acid (0.2 M in DMF), 1 mL of HBTU (0.5 M in DMF), and 0.5 mL DIPEA (2 M in NMP) were added to the reaction vessel. Since chlorotrityl resin is not robust at high temperatures, 50 °C microwave methods were used. Arg was double coupled. All amino acids were deprotected twice with 7 mL of 20% piperidine in DMF. HOBT was not used in the deprotection because it can undergo undesirable side reactions with chlorotrityl resin. The resin was washed extensively between each cycle.

Before removal of the Fmoc-group from Ser₂, the resin beads were removed from the synthesizer, divided into 2 equal portions, and transferred to clean RVs for the final coupling of either Boc-L-Leu-OH or Boc-L-thionoleucylalanine-1-(6-nitro)benzotriazolide using the manual synthesis protocol described above. The resin beads were dried and then incubated on a rotisserie twice for 60 min with 6 mL portions of fresh TFA/H₂O/TIPS (38:1:1 v/v). After each

incubation period, the cleavage cocktail for each peptide was expelled from the RV with nitrogen and dried by rotary evaporation. The residue was diluted to 10 mL with CH₃CN/H₂O (3:2 v/v) before purification. Crude peptides were purified by reverse-phase HPLC with linear H₂O/CH₃CN solvent gradients that maintained 98% aqueous phase over 6 minutes, then ramped from 98% to 50% aqueous phase over 24 min, then to 0% aqueous phase over 5 min, followed by a 10 min wash out period, during which the solvent system returned to 98% aqueous phase. Using this method, the peptides eluted at 26-27 min (Fig. S1). Peptides were analyzed by MALDI-MS (Table S1).

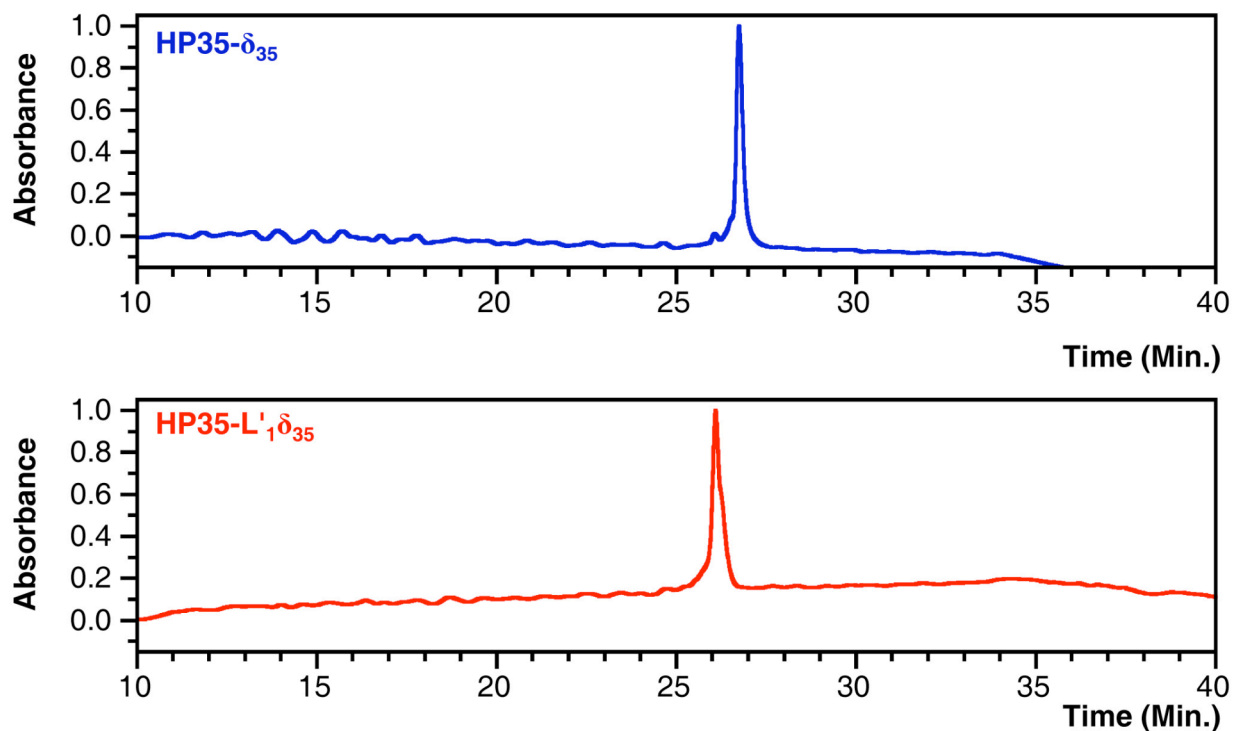


Figure S1. Analytical HPLC Chromatograms of Purified Peptides. Top: HP35-δ₃₅ monitored at 215 nm. Bottom: HP35-L'₁δ₃₅ monitored at 215 nm. Absorbance is normalized. Solvent gradients given in text.

Table S1. Calculated and Observed Peptide Masses.

Peptide	Calculated m/z [M+H] ⁺	Observed m/z [M+H] ⁺	Calculated m/z [M+Na] ⁺	Observed m/z [M+Na] ⁺
LP ₂ ω	513.28	513.40	535.26	535.35
L'P ₂ ω	529.26	529.38	551.24	551.32
LG ₂ ω	433.22	433.22	455.20	455.23
L'G ₂ ω	449.20	449.19	471.18	471.20
LP ₂ μ	571.28	571.24	593.26	593.22
L'P ₂ μ	587.25	587.24	609.24	609.21
LG ₂ μ	491.21	491.26	513.20	513.34
L'G ₂ μ	507.19	507.29	529.17	529.30
LP ₂ δ	590.30	-	612.28	612.08
L'P ₂ δ	606.27	-	628.26	628.10
LP ₂ δ-NH ₂	589.31	589.14	611.30	611.13
L'P ₂ δ-NH ₂	605.29	-	627.27	627.09
LG ₂ δ	510.23	510.23	532.22	532.02
L'G ₂ δ	526.21	526.32	548.19	548.27
HP35-δ ₃₅	4174.16	4174.64	4196.14	-
HP35-L' ₁ δ ₃₅	4190.14	4190.91	4212.12	-

Fluorescence Spectroscopy. UV/visible absorbance spectra were acquired for all peptide and fluorophore solutions. Concentrations were determined using literature values for the extinction coefficients of 7Aw ($\epsilon_{290} = 6,700 \text{ M}^{-1}\cdot\text{cm}^{-1}$), Mcm ($\epsilon_{324} = 12,000 \text{ M}^{-1}\cdot\text{cm}^{-1}$), and Acd ($\epsilon_{386} = 5,700 \text{ M}^{-1}\cdot\text{cm}^{-1}$).^{S3-5} Fluorescence measurements in the presence and absence of 50 mM acetamide or 50 mM thioacetamide were conducted for each fluorophore (7Aw, 7-methoxycoumarin, and Acd) in 100 mM sodium phosphate buffer, pH 7.00. For each fluorophore, samples were prepared by diluting a concentrated stock with additional buffer and 100 mM solutions of

acetamide or thioacetamide in buffer such that all solutions of a given fluorophore were equimolar in concentration. Corrected fluorescence spectra were collected as the average of three scans at 25 °C of three samples of each solution using quartz fluorometer cells with path lengths of 1.00 cm. Fluorophores were excited at 305 nm for 7Aw, 325 nm for 7-methoxycoumarin, and 386 nm for Acd. The excitation and emission slit widths were 5 nm, the scan rate 120 nm/min, the averaging time 0.500 s, and the data interval 1.0 nm. Examples of fluorescence spectra are shown in Figure S2.

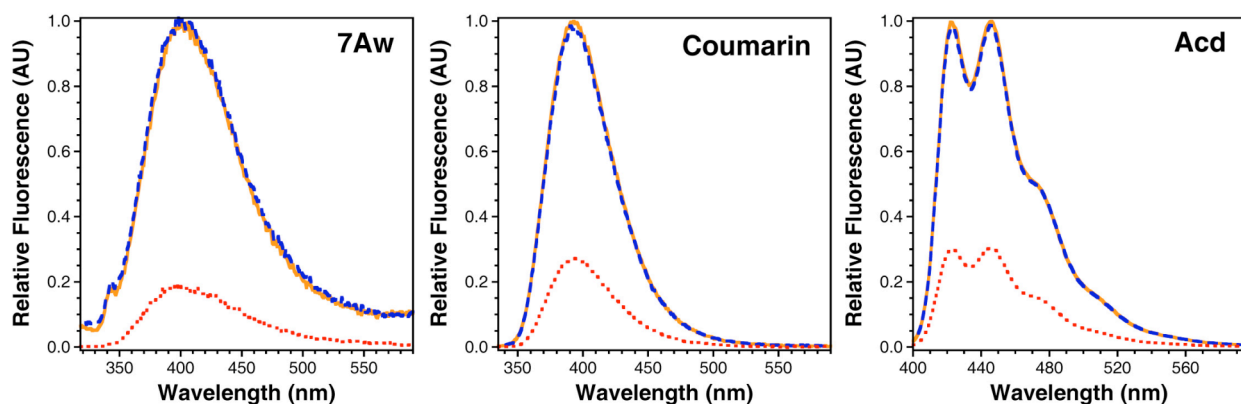


Figure S2. Thioacetamide Quenching of Fluorophores. Representative fluorescence spectra of 41 μM 7Aw (left), 8.9 μM 7-methoxycoumarin (center), and 3.7 μM Acd (right) in 100 mM sodium phosphate buffer, pH 7.00 (solid orange trace); in the presence of 50 mM acetamide (dashed blue trace); and in the presence of 50 mM thioacetamide (dotted red trace).

The quenching efficiency (E_Q) of aqueous thioacetamide was calculated using Equation S1.

$$E_Q = 1 - (F/F_0) \quad (\text{S1})$$

Here, F_0 is the fluorescence intensity of the fluorophore at the wavelength of maximum emission in the absence of thioacetamide (that is, in 100 mM phosphate buffer) and F is the corresponding fluorescence intensity at the same wavelength in the presence of 50 mM thioacetamide. Reported E_Q values are the average of three trials.

Dry proline and glycine peptides were brought up in a minimal volume of pH 7.0 phosphate buffered saline (PBS: 10 mM Na₂HPO₄, 150 mM NaCl, pH adjusted with HCl). For each set of oxo- and thiopeptides, the solutions were diluted to uniform concentration with an absorbance of approximately 0.1 or less at the appropriate excitation wavelength: 305 nm for 7Aw, 325 nm for Mcm, and 386 nm for Acd. Corrected fluorescence spectra were collected at 25 °C on three samples of each peptide using quartz fluorometer cells with path lengths of 1.00 cm and averaging over three scans per sample. Examples of fluorescence spectra and associated UV spectra are shown in Figure S3.

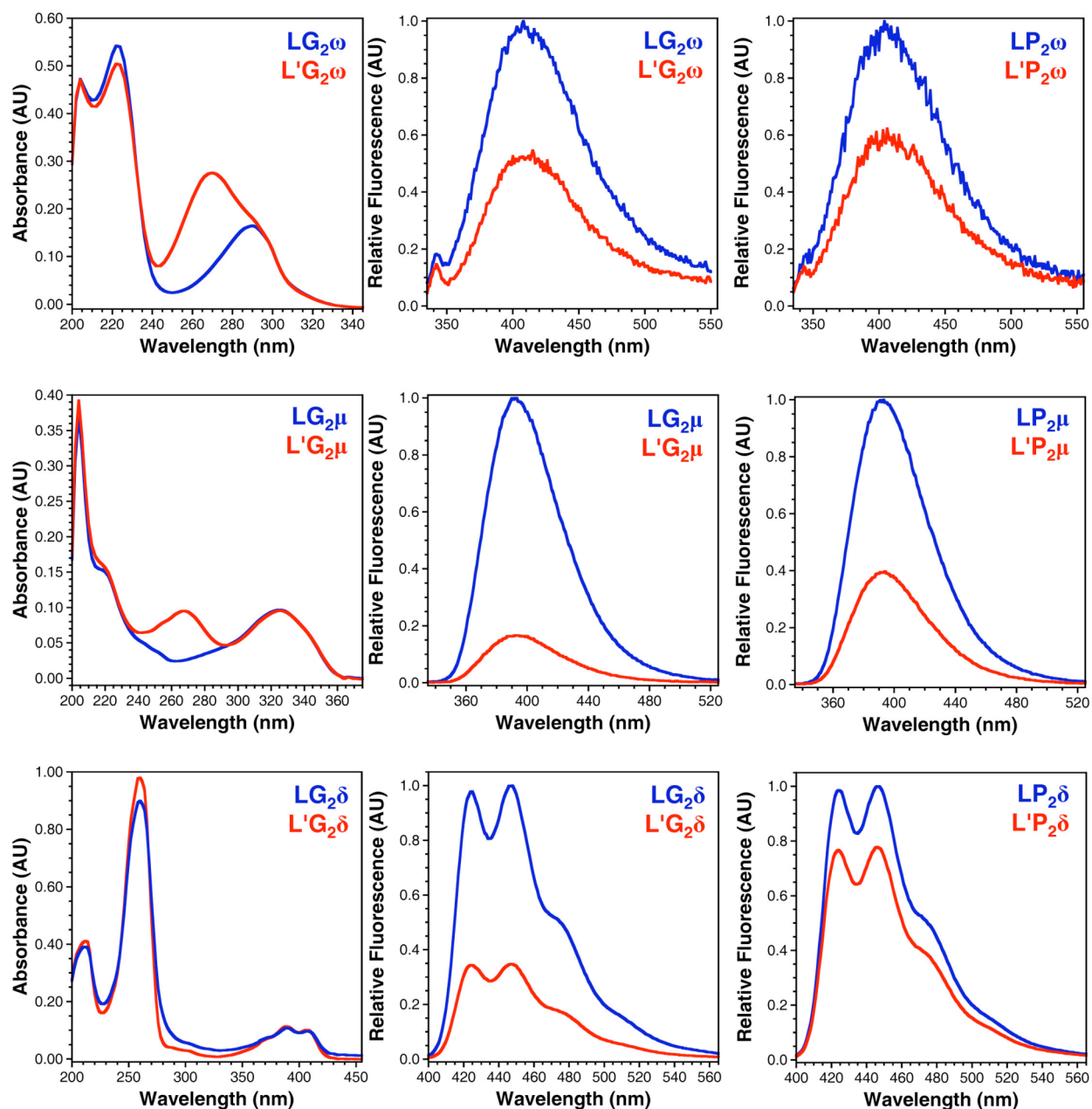


Figure S3. UV/Vis and Fluorescence Spectra of Proline and Glycine Peptides. Representative spectra of oxo-peptides (blue) and thiopeptides (red) containing 7Aw (top), Mcm (middle), and Acd (bottom) in PBS. From Left: Background-corrected absorbance spectra of glycyll peptides and concentration-corrected, normalized fluorescence spectra of glycyll and prolyl peptides.

The thioamide quenching efficiency (E_Q) was determined by comparing the concentration-corrected fluorescence of each peptide using Equation S1, where F_0 was the normalized fluorescence intensity at maximum emission of the oxopeptide and F was the normalized fluorescence intensity at the same wavelength of the thiopeptide.

Acid Stern-Volmer Experiments. Stocks of 116 μM Acd and 100 mM thioacetamide in 100 mM sodium phosphate buffer, pH 7.00, were used to prepare samples that were uniform in Acd concentration (ca. 3.5 μM) and variable in thioacetamide concentration (0, 2.5, 5, 15, 25, 35, 50, and 65 mM). The fluorescence of each sample was measured by exciting the solution at 387 nm and recording the emission from 400 to 600 nm at a 1.0 nm data pitch with a 0.100 s averaging time and a 5 nm slit width, then averaging the corrected spectra of three scans (Fig. S4). Measurements were made in 1.00 cm quartz cuvettes with stirring at 10, 25, 35, 45, and 65 $^\circ\text{C}$ (Fig. S4). The samples were allowed to equilibrate for several minutes at each temperature before scans were taken. The fluorescence intensity at 450 nm was averaged from three separate trials to obtain values for Stern-Volmer calculations. The data for a given temperature were fit to Equation S2 with KaleidaGraph (Synergy Software; Reading, PA).

$$\frac{F_0}{F} = 1 + K_{\text{sv}}[Q] \quad (\text{S2})$$

F_0 is the average fluorescence intensity at 450 nm in the absence of quencher; F is the fluorescence intensity at 450 nm at each thioacetamide concentration step; K_{sv} is the Stern-Volmer constant in M^{-1} ; and $[Q]$ is the concentration of the quencher (thioacetamide) in M (Fig. S4).

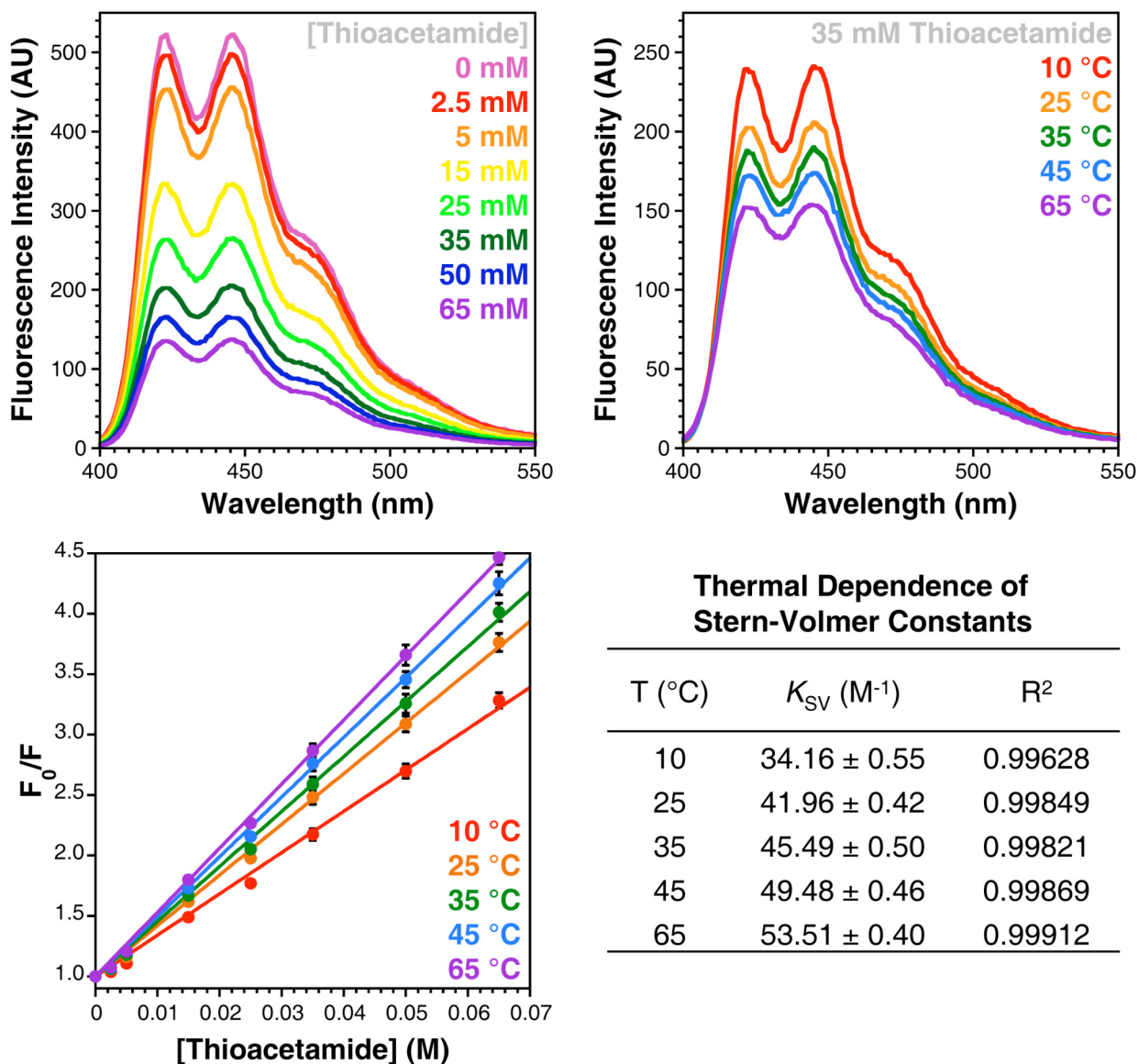


Figure S4. Steady-State Stern-Volmer Experiments. Upper Left: Acridine fluorescence with varying concentrations of thioacetamide in 100 mM sodium phosphate buffer, pH 7.00 at 25 °C ($\lambda_{ex} = 387$ nm). Upper Right: Fluorescence spectra of 3.5 μ M Acridine with 35 mM thioacetamide in buffer at several temperatures. Lower Left: Stern-Volmer plots of thioacetamide quenching Acridine at several temperatures. Error bars are calculated from standard error. Lower Right: Stern-Volmer constants and goodness-of-fit values at each temperature for the fits of Equation S2.

Fluorescence Lifetime Measurements. Fresh solutions of each sample, as well as a solution of 3.5 μM Acd and 50 mM acetamide in buffer, were prepared at identical concentrations for Stern-Volmer lifetime experiments. Time-resolved fluorescence measurements were performed using the Time-Correlated Single Photon Counting (TCSPC) method. The TCSPC system consisted of a blue diode laser (PicoQuant GmbH; Berlin, Germany) generating 10 MHz output pulses at 405 nm, a subtractive double monochromator with an MCP-PMT (Hamamatsu Photonics R2809U; Bridgewater, NJ), and a TCSPC computer board (Becker and Hickl SPC-630; Berlin, Germany). Emission at 450 nm was monitored. All samples were thermostatted at 25 $^{\circ}\text{C}$ in water-jacketed cuvettes. Data analysis was performed with FluoFit software (Picoquant) using a single-exponential decay model (Eq. S3).

$$I(t) = \sum_{i=1}^n A_i e^{-\frac{t}{\tau_i}} \quad (\text{S3})$$

Here, $n = 1$, for a single-exponential fit, and the parameters A_i and τ_i are the amplitude and lifetime of the i^{th} component, respectively. Reduced χ^2 values were calculated for each fit according to Equation S4.

$$\chi^2 = \frac{1}{N-p} \sum_{j=1}^N W(j)^2 [\text{decay}(j) - \text{fit}(j)]^2 \quad W(j) = \frac{1}{\sqrt{\text{decay}(j)}} \quad (\text{S4})$$

In this equation, N is the number of fitted data points j (i.e. measured photon counts at a given delay time, a bin); p is the number of adjustable, fitted parameters; $W(j)$ is a Poisson weighting factor; $\text{decay}(j)$ is the experimentally determined decay curve; and $\text{fit}(j)$ is the fitted model. The residuals were calculated according to Equation S5 using these values.

$$R = W(j)[\text{decay}(j) - \text{fit}(j)] \quad (\text{S5})$$

Representative fits and their corresponding residual plots are shown in Figure S5.

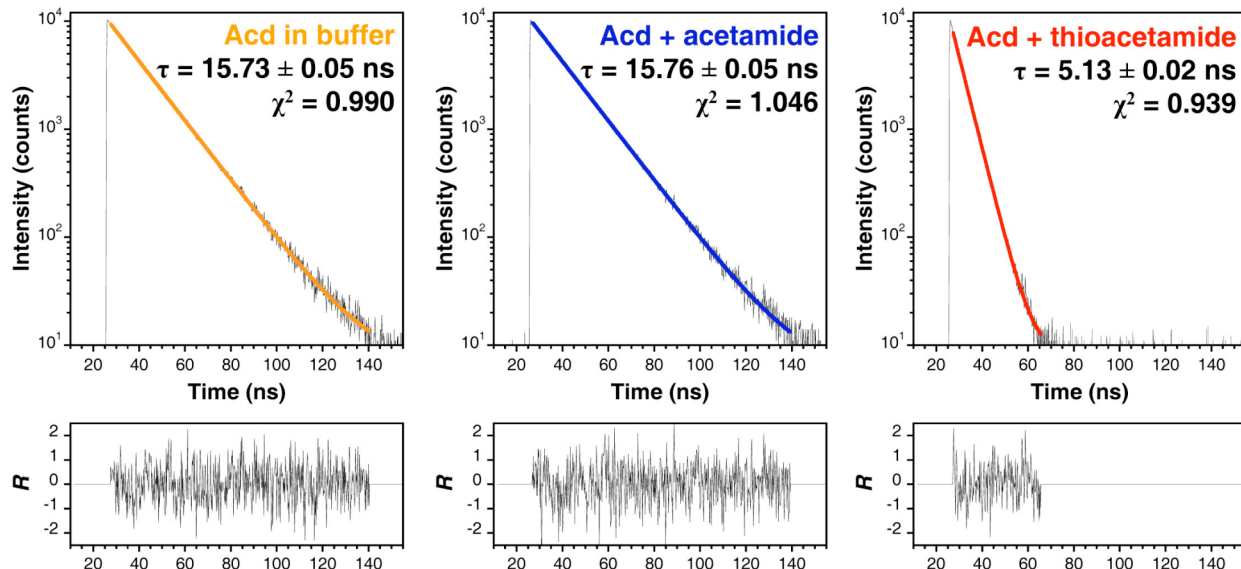


Figure S5. Acd Fluorescence Lifetime Measurements. Left: 3.5 μM Acd in 100 mM sodium phosphate buffer, pH 7.00. Center: 3.5 μM Acd and 50 mM acetamide in buffer. Left: 3.5 μM Acd and 50 mM thioacetamide in buffer. All measurements were made at 25 $^{\circ}\text{C}$ ($\lambda_{\text{ex}} = 405 \text{ nm}$; $\lambda_{\text{em}} = 450 \text{ nm}$). Colored lines are single exponential fits to the data. Lifetimes and reduced χ^2 values are given in the upper right corner of each plot. Residuals are shown beneath each trace.

The Acd fluorescence lifetime data were used to construct a Stern-Volmer plot according to Equation S6

$$\frac{\tau_0}{\tau} = 1 + K_{\text{SV}}[Q] \quad (\text{S6})$$

where τ_0 is the fluorescence lifetime in the absence of quencher ($15.73 \pm 0.05 \text{ ns}$); τ is the fluorescence lifetime at each thioacetamide concentration step; K_{SV} is the Stern-Volmer constant in units of M^{-1} ; and $[Q]$ is the concentration of the quencher (thioacetamide) in M (Fig. S6). Using this equation, we found $K_{\text{SV}} = 41.36 \pm 0.05 \text{ M}^{-1}$. The quenching rate constant, $k_{\text{Q}} = 2.6 \times 10^9 \text{ M}^{-1}\text{s}^{-1}$, was calculated using Equation S7.

$$K_{\text{SV}} = k_{\text{Q}}\tau_0 \quad (\text{S7})$$

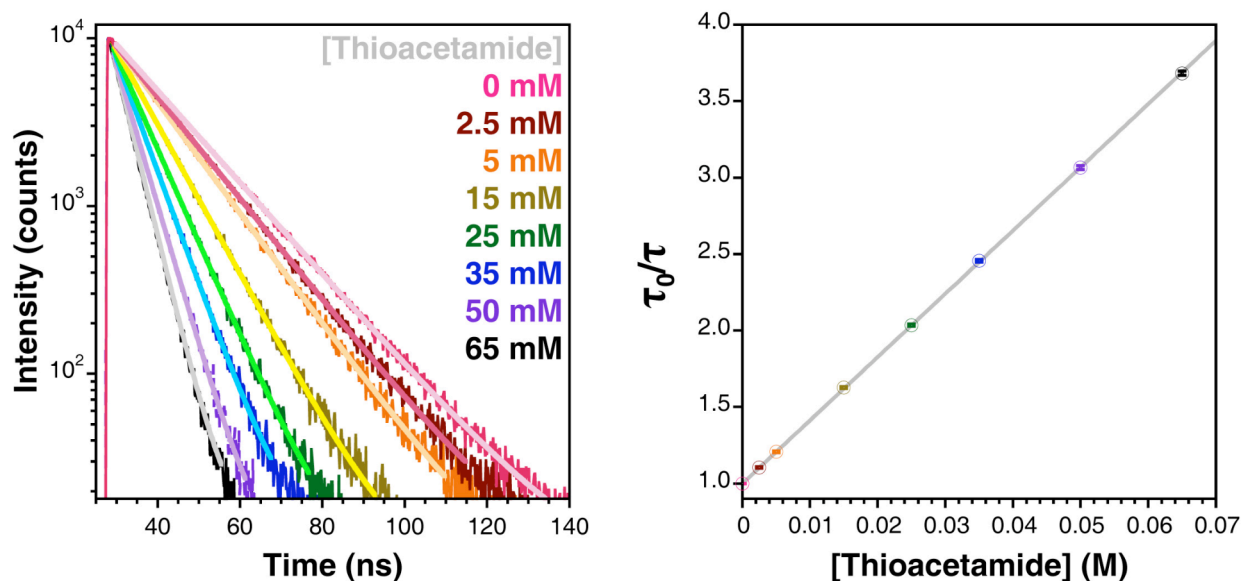


Figure S6. Lifetime Stern-Volmer experiments. Left: Fits to normalized Acd fluorescence lifetime data with varying concentrations of thioacetamide in 100 mM sodium phosphate buffer, pH 7.00 ($\lambda_{\text{ex}} = 405$ nm; $\lambda_{\text{em}} = 450$ nm). Right: Stern-Volmer plot of lifetime data at 25 °C. Error bars are calculated from fits of the raw data; $R^2 = 0.99997$.

Smoluchowski Equation Calculations. A value for the theoretical bimolecular collision quenching constant can be calculated by approximating the fluorophore and quencher to be hard spheres with radii R_A and R_B , respectively, colliding in solution with a rate constant given by

$$k_2 = \frac{2RT}{3\eta} \left(\frac{(R_A + R_B)^2}{R_A R_B} \right) (1000) \quad (\text{S8})$$

where $R = 8.3145 \text{ kg}\cdot\text{m}^2\cdot\text{s}^{-2}\cdot\text{K}^{-1}\cdot\text{mol}^{-1}$ is the ideal gas constant, T is the temperature (in K) of the solution, η is the viscosity of the solvent, and 1000 is a conversion factor to relate L and m^3 .^{S6} A viscosity of $9.314 \times 10^{-4} \text{ kg}\cdot\text{m}^{-1}\cdot\text{s}^{-1}$ was used for 100 mM sodium phosphate solution at 298 K.^{S7} The radii of Acd (R_A) and thioacetamide (R_B) were estimated from the equilibrium geometries calculated for each molecule using the AM1 semi-empirical method in Spartan (Wavefunction, Inc.; Irvine, CA) (Fig. S7). The Acd diameter (15.154 Å) was computed as the sum of the H6 to H12 distance and twice the van der Waals radius of hydrogen (1.200 Å).^{S8} The molecular van der Waals radius ($R_A = 7.577$ Å) was taken to be half of this value. For thioacetamide, the

diameter (6.699 Å) was calculated as the sum of the S1 to H4 distance and the van der Waals radii of sulfur (1.851 Å) and hydrogen.^{S8} The molecular van der Waals radius (3.350 Å) was computed as half of this value. Using these results, we calculated $k_2 = 8.3 \times 10^9 \text{ M}^{-1} \text{ s}^{-1}$. This value is similar in magnitude to the experimentally determined value of $k_Q = 2.6 \times 10^9 \text{ M}^{-1} \text{ s}^{-1}$. The discrepancy between these values can be attributed to a quenching efficiency factor $f_Q = k_Q/k_2 = 0.31$ that accounts for the possibility that not all collisions may result in quenching. It is also possible to attribute the difference between k_2 and k_Q to the coarseness of the approximations in the model.

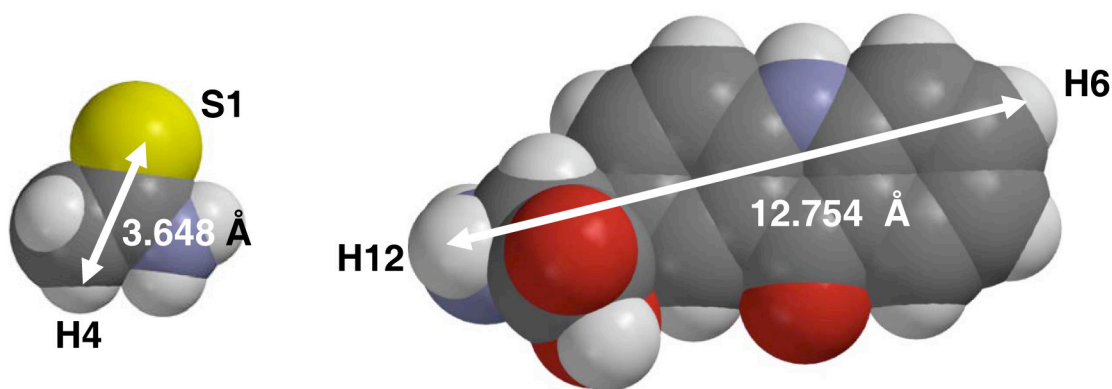


Figure S7. Equilibrium Geometries of Thioacetamide and Acd. Left: Thioacetamide S1 to H4 distance. Right: Acd H6 to H12 distance. Distances calculated in Spartan using geometries optimized at the AM1 level of theory.

Thioacetamide and Acd Absorbance Spectroscopy. UV-visible spectra were acquired of dilute (6.7 μM) and concentrated (266 μM) solutions of Acd in 100 mM sodium phosphate buffer that contained 50 mM thioacetamide. These spectra were compared to spectra of 50 mM thioacetamide in 100 mM phosphate buffer and to spectra of equimolar solutions of Acd in buffer. After correcting for thioacetamide absorbance, no difference was observed between the spectra of solutions that contained thioacetamide and those that did not. This observation suggests that Acd and thioacetamide do not form a ground-state complex with unusual optical

characteristics, which would have been indicative of a static-quenching mechanism. Representative spectra are shown in Figure S8.

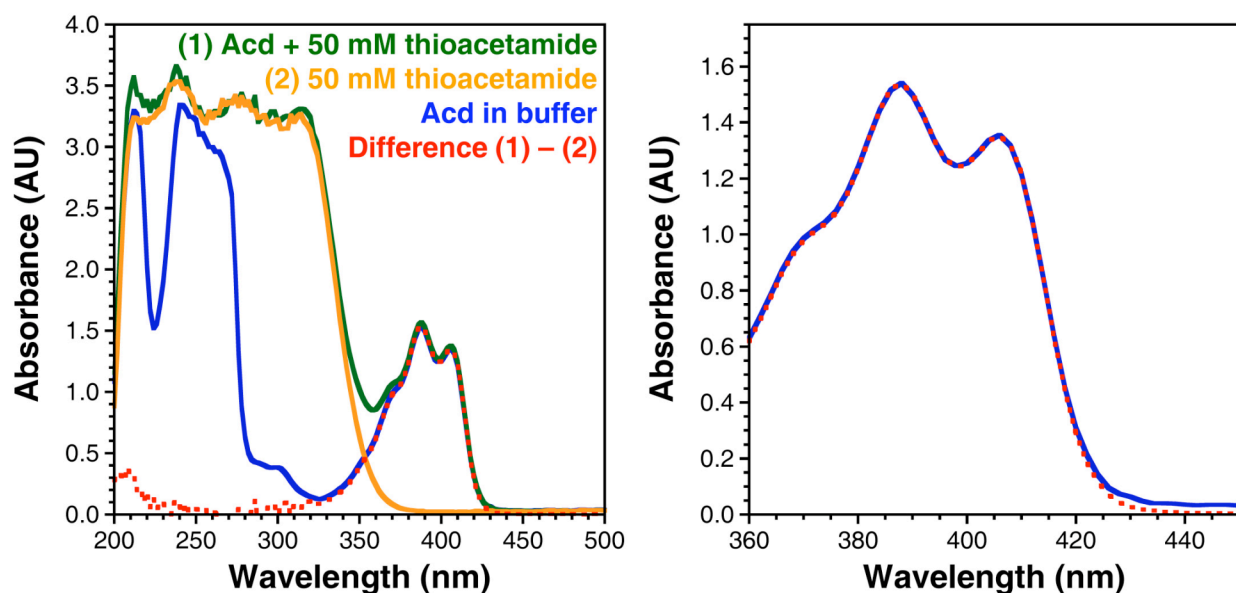


Figure S8. Representative Absorbance Spectra of Acd and Thioacetamide. Left: UV-visible spectra of (1) 266 μM Acd and 50 mM thioacetamide in 100 mM sodium phosphate buffer, pH 7.00 (green trace); (2) 50 mM thioacetamide in buffer (orange trace); and 266 μM Acd in buffer (blue trace). The difference spectrum of (1) and (2) is shown as a dotted red trace. Right: Comparison of the spectrum of 266 μM Acd (solid blue trace) and the difference spectrum of (1) and (2) (dotted red trace) from 360 to 450 nm.

Electrochemical Measurements and Calculations. Cyclic voltammetry measurements were made using a CHI 620D electrochemical analyzer/workstation (CH Instruments; Austin, TX) and data were processed with CHI software v. 9.24. All measurements were made in dry DMF under an N_2 atmosphere with 100 mM tetrabutylammonium hexafluorophosphate (TBAPF_6) as a supporting electrolyte. The cell consisted of a platinum disc (2 mm diameter) working electrode, a platinum wire counter electrode, and a silver wire plated with AgCl as a quasi-reference electrode in a glass vial. Potentials were calibrated to a ferrocene standard, which was added at the end of each run, and reported versus SCE (Fig. S9).^{S9,10}

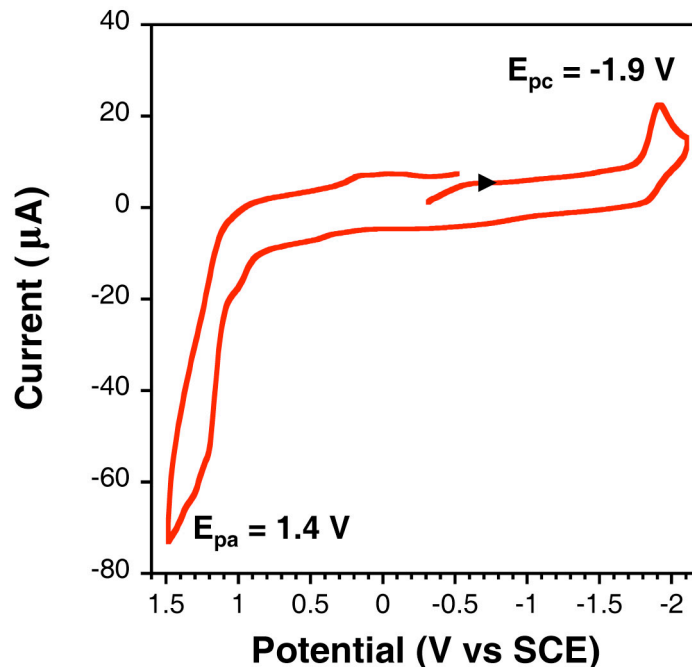


Figure S9. Cyclic Voltammogram of 1 mM Acridone in DMF. Arrow indicates scan direction. Potentials referenced to SCE through a ferrocene standard as described in the text. Scans acquired at 0.5 V/s and at a sample interval of 0.01 V. Anodic (E_{pa}) and cathodic (E_{pc}) peak potentials are indicated.

The Gibbs free energy of photo-induced electron transfer (ΔG_{ET}) is given by Equation S9^{S11}

$$\Delta G_{ET} = N_A e (E_{D^+/D}^\circ - E_{A/A^-}^\circ) - E_{0,0} + C \quad (S9)$$

where N_A is Avogadro's number; e is the elementary charge; $E_{D^+/D}^\circ$ and E_{A/A^-}° are the standard electrode potentials of the donor and acceptor moieties, respectively; C is a solvent-dependent term accounting for the electrostatic work arising from the Coulombic interaction between the donor and acceptor during electron transfer, which is typically negligible in polar solvents; and $E_{0,0}$ is the vibrational zero electronic energy of the excited chromophore calculated as

$$E_{0,0} = \frac{E_{abs} + E_{em}}{2} \quad (S10)$$

Here E_{abs} and E_{em} are the energies corresponding to the wavelengths of absorption and emission of the fluorescent transition being observed. In the case of acridone, there are two relevant absorption wavelengths (388 nm and 406 nm) and there are two relevant emission wavelengths

(422 nm and 446 nm). Using these wavelengths, we take the average value $E_{0,0} = 3.0$ eV. Bordwell and coworkers report the oxidation potential of thioacetamide as 1.21 V *vs.* SHE (0.97 V *vs.* SCE).^{S12} Substituting these values into Equation S9, we find $\Delta G_{ET} = -0.13$ eV = -12.5 kJ/mol. This general approach can be extended to 7-methoxycoumarin, for which the reduction potential is -1.91 V *vs.* SCE and $E_{0,0} = 3.48$ eV.^{S13} Substituting these values into Equation S9, we find $\Delta G_{ET} = -0.6$ eV for thioamide quenching of coumarin. We note that these treatments assume thioacetamide to be acting as the electron donor and the fluorophore to be acting as the electron acceptor. It may also be possible for the donor and acceptor roles to be reversed; further experiments are required to completely elucidate the mechanism.

Circular Dichroism Measurements. Circular dichroism (CD) spectroscopy on HP35- δ_{35} and HP35-L' δ_{35} was used to ensure that both proteins adopted a folded structure at 25 °C and to determine the T_m s of each protein, as well as the fraction of protein in a folded state as a function of temperature. CD measurements were made on approximately 50 μ M solutions of the proteins in 10 mM sodium phosphate, 150 mM NaCl, pH 7.00. Wavelength scans were collected at 25 °C from 280 nm to 200 nm with a 1 nm data pitch and a 10 s averaging time. Thermal scans were collected at 222 nm between 1 and 97 °C using the variable temperature module provided with the Aviv 410 CD spectrometer. Data were collected with a 1 °C/min temperature slope, 10 s averaging time, 2 min temperature equilibration time, and 1 nm band width. For both data sets, the resulting raw ellipticity (θ_D) measurements were transformed to molar residue ellipticity values (θ) using

$$\theta = \theta_D / (c \ell n_R) \quad (\text{S11})$$

where c is concentration (M), ℓ is the path length (cm), and n_R is the number of residues (Fig. S10). To determine fraction folded (f_f), linear baselines were fit to the low temperature ($\theta_F = m_F T + b_F$) or high temperature ($\theta_U = m_U T + b_U$) data. The full data range was then fit to equation

S12 where $K = e^{-(\Delta H - T\Delta S)/RT}$, ΔH and ΔS are adjustable parameters and $R = 8.3145 \text{ J}\cdot\text{mol}^{-1}\cdot\text{K}^{-1}$.

Plots are shown for each protein in Figure S10.

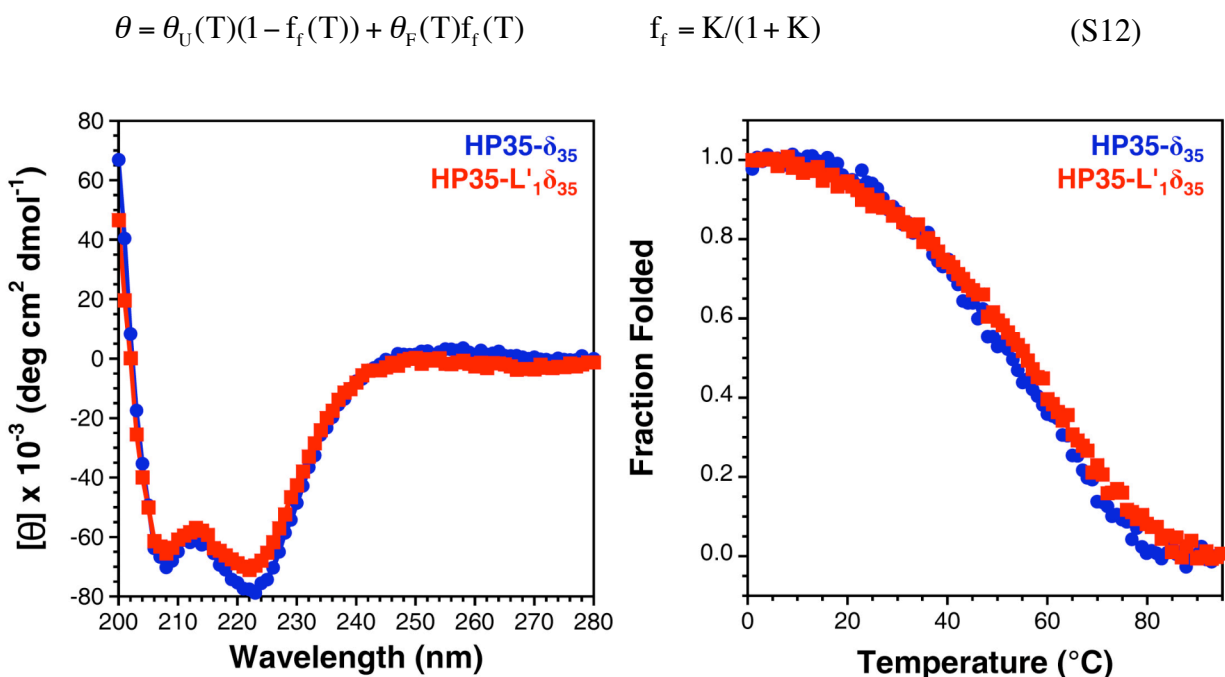


Figure S10. Wavelength and Temperature-Dependent Circular Dichroism Spectroscopy of HP35 proteins. Left: Wavelength scans of $47 \mu\text{M}$ HP35- δ_{35} (blue circles) and $51 \mu\text{M}$ HP35-L' $_1\delta_{35}$ (red squares) in 10 mM sodium phosphate, 150 mM NaCl, pH 7.00 at 25 $^{\circ}\text{C}$. Right: Fraction folded as a function of temperature as determined by molar residue ellipticity (θ) at 222 nm.

HP35 Fluorescence Measurements. All fluorescence measurements were made on dilute solutions of HP35- δ_{35} and HP35-L' $_1\delta_{35}$ in PBS (10 mM sodium phosphate, 150 mM NaCl, pH 7.00). Steady-state emission was monitored at 424 nm and 446 nm with an excitation wavelength of 386 nm. Stirred samples were heated from 1 $^{\circ}\text{C}$ to 95 $^{\circ}\text{C}$ at a rate of 0.25 $^{\circ}\text{C min}^{-1}$ and scans were taken at 0.5 $^{\circ}\text{C}$ intervals with a 0.500 s averaging time. The normalized, concentration-corrected fluorescence intensity at each wavelength was used to calculate quenching efficiency using Equation S1 where F_0 was the fluorescence intensity of HP35- δ_{35} and F was the fluorescence intensity of HP35-L' $_1\delta_{35}$ (Fig. S11). The thermal dependence of the

quenching efficiency was identical at 424 and 446 nm. This data was used to construct Fig. 3 in the main text as shown in Figure S12.

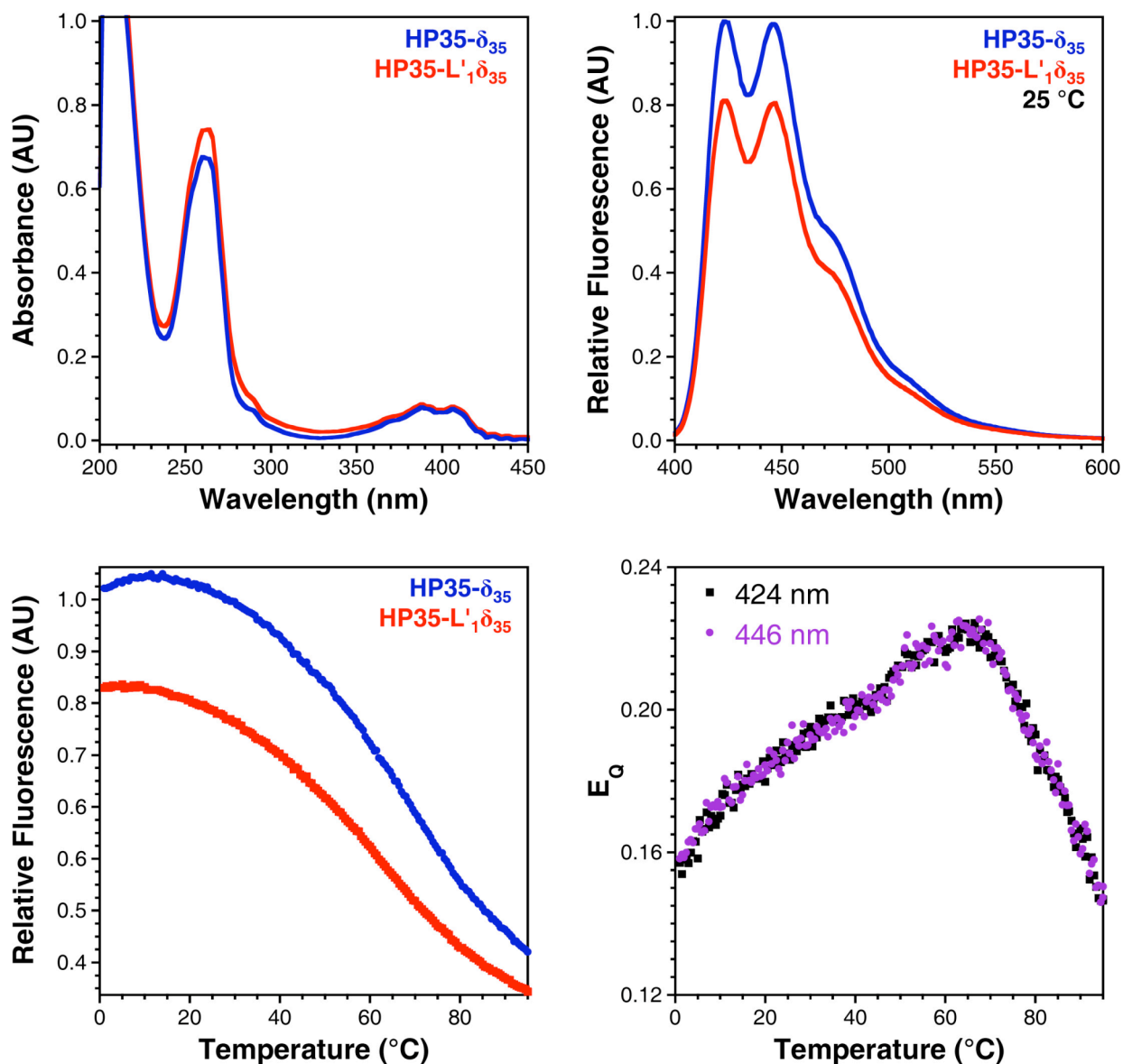


Figure S11. Temperature-Dependent Fluorescence Spectroscopy of HP35 proteins. Upper Left: Background-corrected UV-visible absorbance spectra of 14 μM HP35- δ_{35} (blue trace) and 15 μM HP35-L' $_1\delta_{35}$ (red trace) in 10 mM sodium phosphate, 150 mM NaCl, pH 7.00. Upper Right: Normalized, concentration-corrected fluorescence spectra of the same solutions at 25 °C ($\lambda_{\text{ex}} = 386$ nm). Lower Left: Normalized, concentration-corrected emission at 424 nm of both solutions as a function of temperature ($\lambda_{\text{ex}} = 386$ nm). Lower Right: Thermal dependence of thioamide quenching efficiency (E_Q) in HP35 proteins determined at 424 nm (black squares) and 446 nm (purple circles) as described in text.

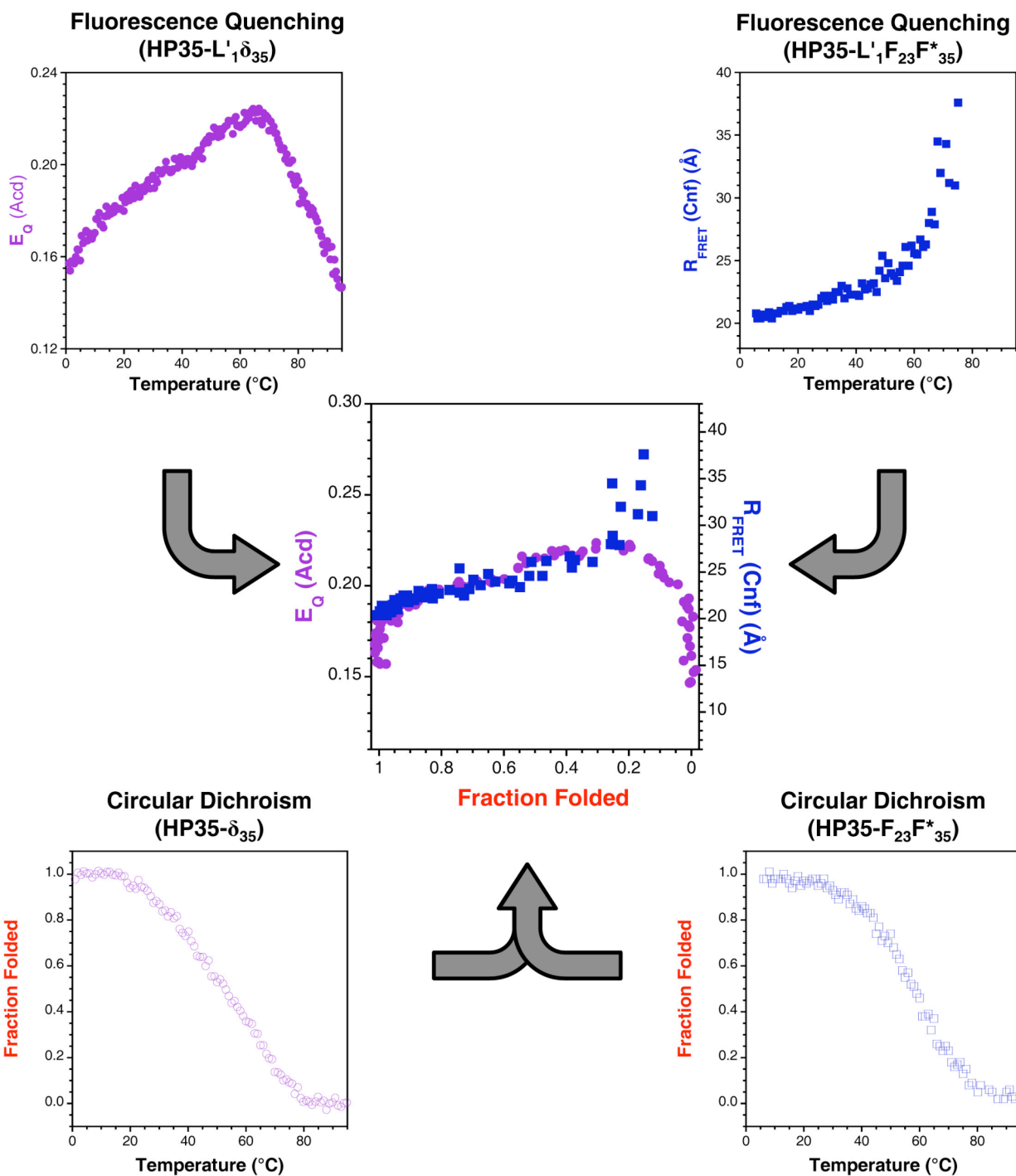


Figure S12. HP35 Data Used to Construct Figure 3. Top Left: Quenching efficiency of HP35- L'₁δ₃₅ as a function of temperature. Top Right: Separation in Å of the N- and C-termini of HP35- L'₁F₂₃F*₃₅ as a function of temperature as determined by Förster Resonance Energy Transfer (FRET) as described in Goldberg *et al.*^{S14} Center: Data from upper panels transformed to be functions of fraction of protein folded by mapping fluorescence data as a function of temperature to the circular dichroism data for HP35- L'₁δ₃₅ (bottom left) and HP35- L'₁F₂₃F*₃₅ (bottom right), as appropriate.

Fluorescence lifetime measurements were made at 10, 25, 40, 55, 70, and 85 °C using the procedure outlined above. Since fits to a single exponential function (Eq. S3, $n = 1$) were not satisfactory, we fit the data to a bi-exponential model (Eq. S3, $n = 2$) and a Gaussian model distributed about a single center lifetime (Eq. S13, $i = 1$).

$$I(t) = \int_{-\infty}^{\infty} \rho(\tau) e^{-\frac{t}{\tau}} d\tau \quad \rho(\tau) = \sum_{i=1}^n \frac{A_i}{\sigma_i \sqrt{2\pi}} e^{-\frac{1}{2} \left(\frac{\tau - \tau_i}{\sigma_i} \right)^2} \quad \sigma_i = \frac{\Delta_{FWHM_i}}{\sqrt{8 \ln 2}} \quad (\text{S13})$$

Here, all parameters are defined with respect to the i^{th} distributed component: A_i is the amplitude in the first fitted channel; τ_i is the center the center lifetime; and Δ_{FWHM_i} is the full width at half maximum of the distribution. Reduced χ^2 values were calculated for each fit according to Equation S4 and weighted residuals were calculated according to Equation S5. Representative data sets are shown in Figure S13.

Both the Gaussian and bi-exponential models described the data well as judged by plots of the weighted residuals and the reduced χ^2 values. Since nearly identical trends in the average fluorescence lifetime of HP35- δ_{35} and HP35-L' δ_{35} with respect to temperature were observed with each model, we used bi-exponential fits to analyze all quenching data (Table S2).

Time-resolved measurements of Acd fluorescence of Leu-Pro₂-Acd (LP₂ δ), Leu'-Pro₂-Acd (L'P₂ δ), Leu-Gly₂-Acd (LG₂ δ), Leu'-Gly₂-Acd (L'G₂ δ), Leu-Pro₂-Acd-NH₂ (LP₂ δ -NH₂) and Leu'-Pro₂-Acd (L'P₂ δ -NH₂) peptides were conducted using the same procedure outlined above. Lifetime data of the oxoamide and thioamide peptides were fit with a mono-exponential model (Equation S3, $n = 1$) and a bi-exponential model (Equation S3, $n = 1$). Reduced χ^2 values and weighted residuals were calculated using Equations S4 and S5, respectively. The best fits obtained fitting the oxoamide data with a bi-exponential model (Equation S3, $n = 2$) were those that used τ_1 from the mono-exponential fit as an initial guess. In this case, no τ_2 component was

found. Forcing the τ_2 component to be non-zero resulted in poorer fits for these data sets as judged by χ^2 analysis. However, the bi-exponential model provided superior fits for the fluorescence lifetime data collected from the thioamide-containing peptides relative to those found assuming a mono-exponential model. Fluorescence lifetime data for L'G₂ δ was fit to Equation S3 ($n = 2$) allowing all parameters to float. We found that this bi-exponential model satisfactorily described the data with $\tau_1 = 13.90 \pm 0.06$ ns (96.7% intensity weighted fraction; 91.4% by amplitude weighting) and $\tau_2 = 5.93 \pm 0.14$ ns (intensity-weighted: 3.3%; amplitude-weighted: 8.6%). Since we found the lifetime for the oxoamide peptide LG₂ δ to be 16.35 ± 0.04 ns, we tried fitting the thioamide peptide data by forcing τ_1 to be 16 ns to better evaluate the possibility of having a two component mixture of quenched (τ_2) and unquenched ($\tau_1 = 16$ ns) fluorophores. In this case, we found that the model still described the data well, but τ_2 increased slightly to 7.57 ± 0.08 ns and its fraction increased significantly (intensity-weighted: 36.5%; amplitude-weighted: 54.8%). These results are more conceptually consistent with those observed in the other studies. The τ_2 lifetime returned by this fit is still reasonable, equivalent to an effective molarity of 50 mM thioamide by comparison to the Stern-Volmer study. The results of these experiments are summarized in Table S2.

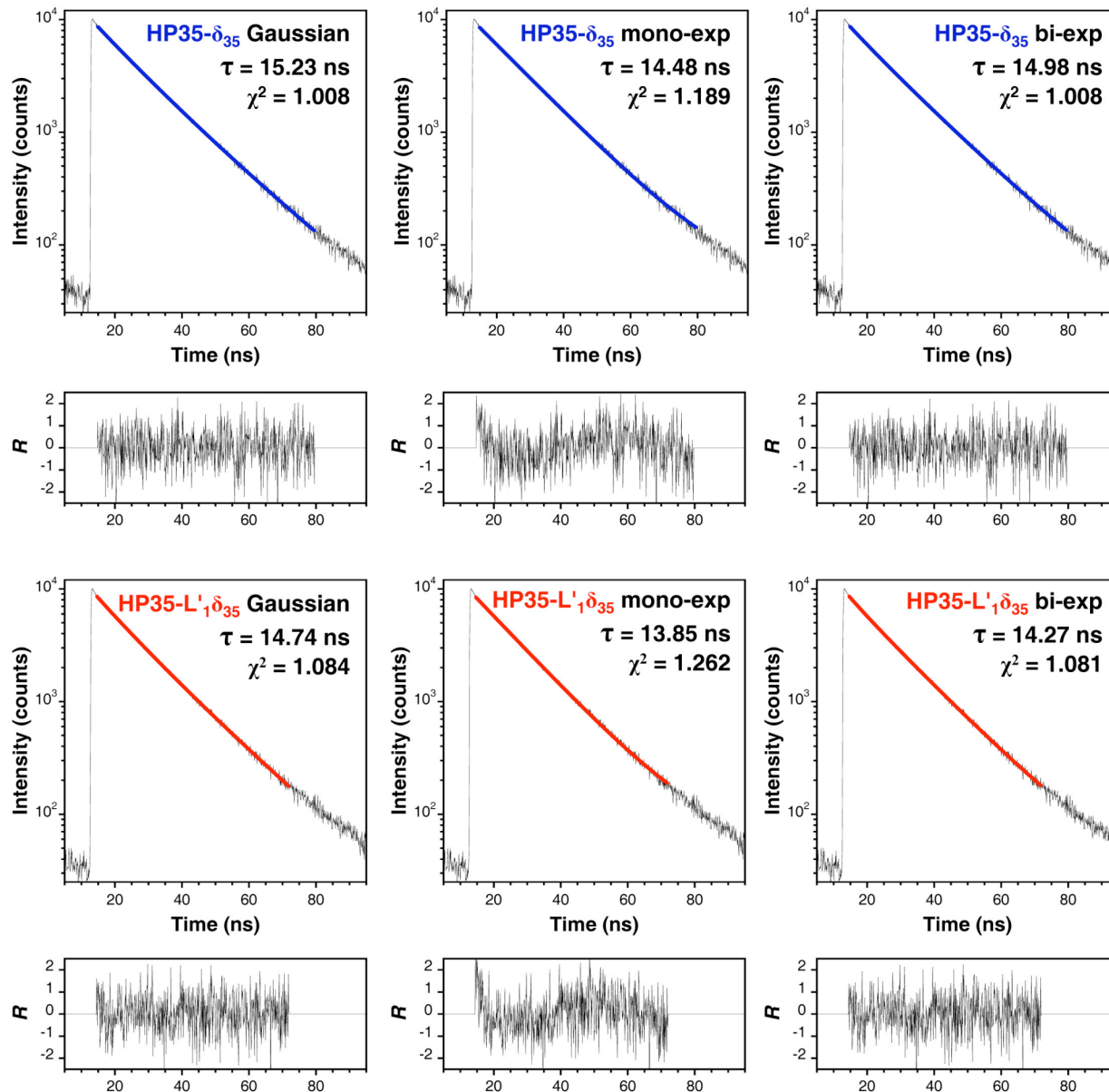


Figure S13. HP35 Fluorescence Lifetime Data at 40 °C Fit to Several Models. Top: Lifetime measurements of 7.9 μ M HP35- δ_{35} in PBS. Bottom: Lifetime measurements of 7.3 μ M HP35-L' $_1\delta_{35}$ in PBS. Colored lines are best fits to Gaussian (left), mono-exponential (center), and bi-exponential (right) models. Weighted residuals are shown beneath each plot. Lifetimes and reduced χ^2 values are shown in the upper right corner of each plot.

Table S2. Fluorescence Lifetime Fitting.

Sample	<i>mono-exponential</i>		<i>bi-exponential</i>					
	τ (ns)	χ^2	τ_{avg} (ns) ^a	χ^2	τ_1 (ns)	A_1 (counts)	τ_2 (ns)	A_2 (counts)
HP35-δ_{35}								
10 °C	16.22 ± 0.05	1.111	16.39 ± 0.28	1.039	16.48 ± 0.05	8505 ± 30	3.40 ± 1.20	306 ± 87
25 °C	15.51 ± 0.05	1.206	15.76 ± 0.25	1.02	15.90 ± 0.05	8824 ± 30	3.26 ± 0.73	501 ± 89
40 °C	14.48 ± 0.05	1.189	14.98 ± 0.20	1.008	15.67 ± 0.05	7269 ± 29	8.17 ± 0.29	1407 ± 49
55 °C	13.01 ± 0.05	1.308	13.54 ± 0.19	1.027	14.12 ± 0.05	7050 ± 28	6.37 ± 0.29	1250 ± 53
70 °C	11.23 ± 0.05	1.561	11.64 ± 0.18	1.027	12.23 ± 0.04	6835 ± 30	5.34 ± 0.23	1466 ± 58
85 °C	9.63 ± 0.05	1.954	9.98 ± 0.15	0.966	10.66 ± 0.04	6847 ± 32	4.67 ± 0.15	1980 ± 61
HP35-L'δ_{35}								
10 °C	15.89 ± 0.05	1.226	16.19 ± 0.26	1.028	16.34 ± 0.05	8589 ± 30	3.25 ± 0.72	506 ± 87
25 °C	15.29 ± 0.05	1.094	15.38 ± 0.24	0.998	15.54 ± 0.05	8318 ± 30	4.58 ± 0.97	408 ± 71
40 °C	13.85 ± 0.05	1.262	14.27 ± 0.21	1.081	14.63 ± 0.05	7787 ± 30	5.87 ± 0.47	833 ± 59
55 °C	12.34 ± 0.05	1.343	12.70 ± 0.19	0.966	13.19 ± 0.04	7277 ± 30	5.58 ± 0.30	1174 ± 58
70 °C	10.75 ± 0.05	1.612	11.11 ± 0.17	0.985	11.64 ± 0.04	6706 ± 30	4.72 ± 0.23	1366 ± 60
85 °C	9.48 ± 0.04	1.799	9.85 ± 0.14	0.95	10.58 ± 0.04	6348 ± 30	4.94 ± 0.14	2029 ± 56
LP$_2$$\delta^b$	16.68 ± 0.05	1.016	16.65 ± 0.05	1.037	16.65 ± 0.05	9048 ± 33	0	0
L'P$_2$$\delta$	15.73 ± 0.05	1.406	16.08 ± 0.28	1.037	16.28 ± 0.05	7640 ± 30	4.50 ± 0.85	483 ± 75
LP$_2$$\delta$-NH$_2^b$	16.67 ± 0.05	0.974	16.6 ± 0.05	0.979	16.66 ± 0.05	9320 ± 32	0	0
L'P$_2$$\delta$-NH$_2$	15.75 ± 0.06	1.403	16.17 ± 0.26	1.049	16.52 ± 0.05	7517 ± 30	6.05 ± 0.63	709 ± 64
LG$_2$$\delta^b$	16.35 ± 0.04	0.882	16.33 ± 0.04	0.901	16.33 ± 0.04	9228 ± 31	0	0
L'G$_2$$\delta$ (Float)^c	11.76 ± 0.08	3.568	12.53 ± 0.19	1.018	13.90 ± 0.06	5188 ± 29	5.93 ± 0.14	2527 ± 59
L'G$_2$$\delta$ (Fit)^d	-	-	12.92 ± 0.16	1.146	16	3735 ± 26	7.57 ± 0.08	4535 ± 52

^a Intensity weighted. ^b Best fits found as described in the text. ^c Best fit parameters floating τ_1 . ^d Best fit parameters constraining $\tau_1 = 16$ ns.

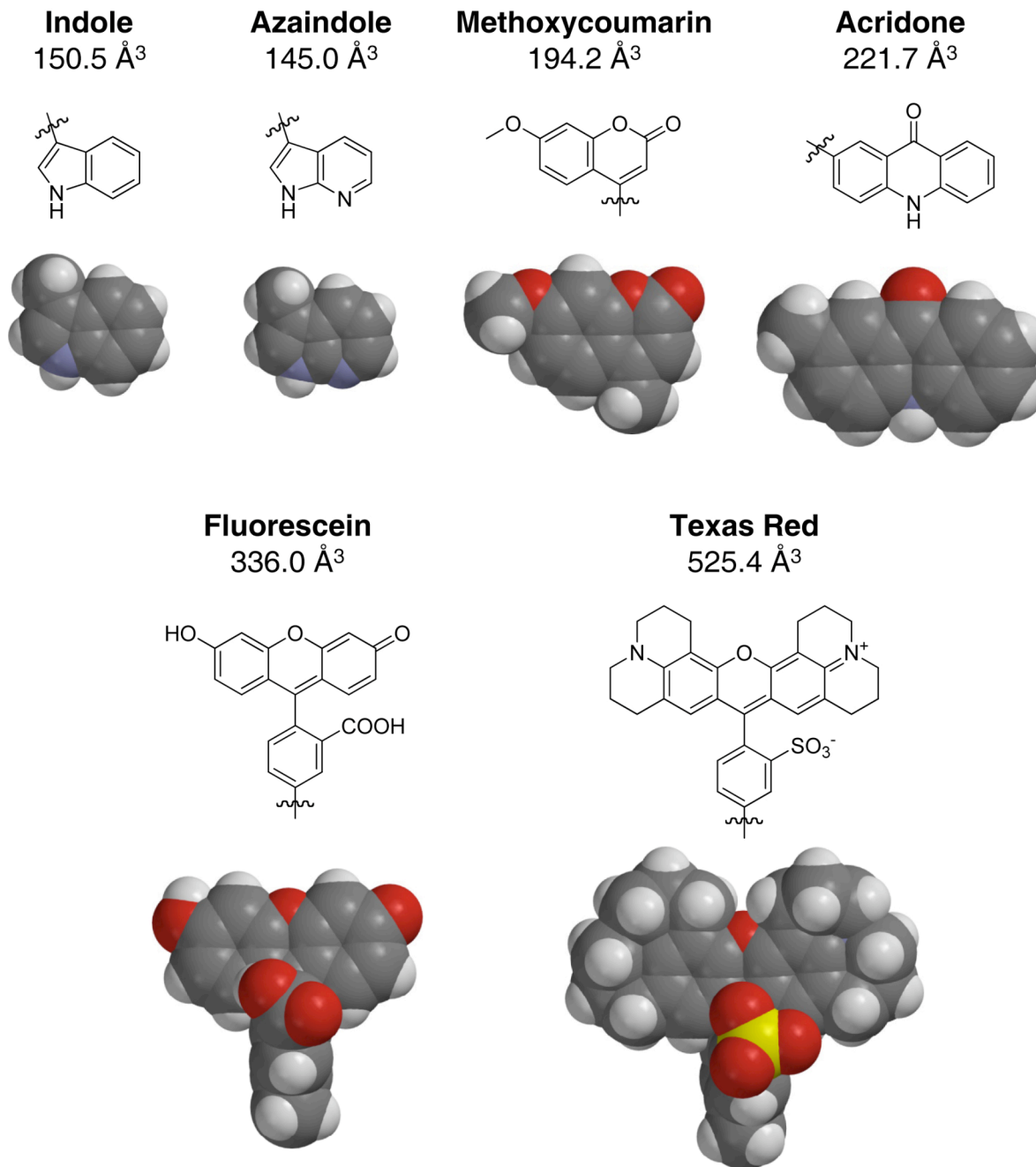


Figure S14. Molecular Volumes of Organic Fluorophores. Geometries optimized at AM1 level and molecular volume calculated using Spartan. Note: The forms of fluorescein and Texas Red shown are truncated relative to commonly used forms. The full forms would only accentuate the size difference relative to acridone and methoxycoumarin.

References

- (S1) Szymanska, A.; Wegner, K.; Lankiewicz, L. *Helv. Chim. Acta* **2003**, *86*, 3326-3331.
- (S2) McKnight, C. J.; Doering, D. S.; Matsudaira, P. T.; Kim, P. S. *J. Mol. Biol.* **1996**, *260*, 126-134.
- (S3) Brun, M. P.; Bischoff, L.; Garbay, C. *Angew. Chem. Int. Ed.* **2004**, *43*, 3432-3436.
- (S4) Hagiwara, Y.; Hasegawa, T.; Shoji, A.; Kuwahara, M.; Ozaki, H.; Sawai, H. *Bioorg. Med. Chem.* **2008**, *16*, 7013-7020.
- (S5) Moran, G. R.; Phillips, R. S.; Fitzpatrick, P. F. *Biochemistry* **1999**, *38*, 16283-16289.
- (S6) Lakowicz, J. R. *Principles of fluorescence spectroscopy*; Springer, 2006.
- (S7) Values for 100 mM sodium phosphate at 298 K estimated from data in Chenlo, F.; Moreira, R.; Pereira, G.; Vazquez, M. J. *J. Chem. Eng. Data* **1996**, *41*, 906-909.
- (S8) Bondi, A. *J. Phys. Chem.* **1964**, *68*, 441-451.
- (S9) Bao, D.; Millare, B.; Xia, W.; Steyer, B. G.; Gerasimenko, A. A.; Ferreira, A.; Contreras, A.; Vullev, V. I. *J. Phys. Chem. A* **2009**, *113*, 1259-1267.
- (S10) Connelly, N. G.; Geiger, W. E. *Chem. Rev.* **1996**, *96*, 877-910.
- (S11) Doose, S.; Neuweiler, H.; Sauer, M. *ChemPhysChem* **2009**, *10*, 1389-1398.
- (S12) Bordwell, F. G.; Algrim, D. J.; Harrelson, J. A. *J. Am. Chem. Soc.* **1988**, *110*, 5903-5904.
- (S13) Seidel, C. A. M.; Schulz, A.; Sauer, M. H. M. *J. Phys. Chem.* **1996**, *100*, 5541-5553.
- (S14) Goldberg, J. M.; Batjargal, S.; Petersson, E. J. *J. Am. Chem. Soc.* **2010**, *132*, 14718-14720.